Running title: Early HPI axis adaptation

Early life challenge enhances cortisol regulation in zebrafish larvae

Luis A. Castillo-Ramírez[1,2], Ulrich Herget[1,3], Soojin Ryu[1,2,4]§, Rodrigo J. De Marco[1,2,5]§

[1]Max Planck Institute for Medical Research, Jahnstr. 29, 69120 Heidelberg, Germany

[2]Developmental Neurobiology of Resilience, German Resilience Center, University Medical Center of the Johannes Gutenberg University Mainz, Duesbergweg 6, 55128 Mainz, Germany

[3]Division of Biology and Biological Engineering, California Institute of Technology, 1200 East California Boulevard, Pasadena, California 91125, USA

[4]Living Systems Institute, College of Medicine and Health, University of Exeter, Stocker Road EX4 4QD Exeter, UK

[5]School of Biological and Environmental Sciences, Faculty of Science, Liverpool John Moores University, Byrom Street, L3 3AF Liverpool, UK

ORCID

Luis A. Castillo-Ramírez https://orcid.org/0009-0005-4896-5586

Ulrich Herget https://orcid.org/0000-0002-4419-1414

Soojin Ryu https://orcid.org/0000-0002-7059-0160

Rodrigo J. De Marco https://orcid.org/0000-0002-2082-4264

§**Authors for correspondence**:

Ryu, Soojin <S.Ryu@exeter.ac.uk>

De Marco, Rodrigo <R.J.DeMarco@ljmu.ac.uk>

Disclosure Statement: The authors have nothing to disclose.

Abstract. The hypothalamic-pituitary-adrenal (HPA) axis in mammals or hypothalamic-pituitary-interrenal (HPI) axis in fish is thought to function as an open system that adapts to the environment during development. We used larval zebrafish to explore how early life challenge (ELC) impacts the early stage of this process. ELC, induced by sustained involuntary swimming at 5 days post-fertilization (dpf), altered subsequent stress responsiveness. At 6 dpf, larvae exposed to ELC showed similar baseline cortisol levels but reduced cortisol reactivity to an initial stressor. Notably, they also showed increased cortisol reactivity to a second stress event within a 30-minute refractory period, when the cortisol response is usually suppressed. Whole-body qPCR revealed upregulation of genes involved in cortisol metabolism and stress modulation, including *hsd11b2*, *cyp11c1*, *star*, *crh*, *oxt*, *crhr1*, *pomca*, *nr3c2*, *nr3c1*, and *fkbp5*. Challenged larvae also showed fewer *crh*-, *avp*-, and *oxt*-positive cells in the nucleus preopticus (NPO), homologous to the mammalian paraventricular nucleus, with diminished co-expression of *crh* and *avp*. Altogether, the results suggest that at the early stage of HPI axis adaptation, ELC optimizes cortisol regulation by preventing excess levels while ensuring adequate release during homotypic stress. Follow-up work should examine the impact of ELC on steroidogenic interrenal cell activity and the maturation of stress circuits in the NPO.

Keywords: Stress axis, Early life challenge, Glucocorticoid reactivity, Cortisol regulation, Developmental programming, Zebrafish larvae

Summary statement: Early life challenge in zebrafish larvae enhances cortisol regulation, preventing excess levels while ensuring adequate production during stress.

Introduction

The HPA/I axis is thought to function as an adaptive system closely linked to the body's response to the environment (Charmandari et al., 2005; Wendelaar Bonga, 1997). As an open system, it is assumed to continuously adjust to the interaction between the organism and its surroundings during development, enhancing its ability to respond to challenges and facilitating effective coping. The larval zebrafish (*Danio rerio*) is a good model for exploring how this process begins due to its genetic accessibility and external development, enabling early-life access (Alsop and Vijayan, 2008; Alsop and Vijayan, 2009; Egan et al., 2009; Champagne and Richardson, 2013; Biran et al., 2015; Eachus et al., 2021; Tan et al., 2022). Stress signals in zebrafish are processed in the NPO, akin to the mammalian paraventricular nucleus (PVN) (Herget et al., 2014), involving key neuropeptides like corticotropin-releasing hormone (CRH). CRH stimulates adrenocorticotropic hormone (ACTH) production in the pituitary gland, leading to glucocorticoid (GC) release, also termed glucocorticoid reactivity (GC_R), from the interrenal gland in fish, similar to the mammalian adrenal gland (Alderman and Bernier, 2009). Glucocorticoids (GCs), such as cortisol, affect metabolism, immunity, reproduction, and behaviour, helping the body cope with challenge (Munck et al., 1984; Chrousos, 1998; de Kloet et al., 1998; de Kloet and Joëls, 2023; McEwen, 2007).

By 4-6 dpf, when their HPI axis becomes functional (Alsop and Vijayan, 2008; Alderman and Bernier, 2009; De Marco et al., 2016), zebrafish larvae in laboratory settings primarily encounter visual cues from conspecifics, as well as mechanosensory inputs from other larvae (unless raised in isolation) and self-generated motion. The temperature and illumination levels of their rearing chambers remain constant, and food availability, if present, can also be controlled. This environment of limited variability provides an opportunity to analyse early HPI axis calibrations to external stimuli. For instance, their response to water currents, where they adjust swimming behaviour to match flow strength, allows for

environments with varying physical challenges. These currents impose significant energy demands on the larvae, leading to different levels of HPI axis activity (Castillo-Ramírez et al., 2019). Using water currents from highly controlled water vortices, we established a high throughput forced swim test for larval zebrafish. This test revealed that ELC, in the form of sustained involuntary swimming, triggers prolonged activation of the HPI axis and alters the cortisol response to a single instance of either homotypic or heterotypic stress 1-4 days after ELC. ELC also enhances spontaneous activity, reduces startle reactivity, and improves energy efficiency during rheotaxis (Castillo-Ramírez et al., 2019). The mechanisms behind these effects remain unknown.

The HPA axis maintains control over its stressor-induced activation levels (Dallman and Yates, 1969; Dallman et al., 1994; Dallman, 2005; Shipston, 2022). In mammals, the PVN is subject to negative feedback inhibition by GCs, resulting in the downregulation of modulators such as *crh* (Malkoski et al., 1999). Given its structural and chemoarchitectural similarity to the mammalian PVN (Herget et al., 2014), it is likely that the zebrafish NPO undergoes similar regulatory feedback mechanisms. This is supported by evidence showing that zebrafish with disrupted GC signalling show an increased number of *crh*-expressing cells in the NPO (Ziv et al., 2012; Facchinello et al., 2017). In mammals, the regulation of the PVN involves not only the expression levels of modulators like *crh* but also the coexpression of several neuropeptides within the same cells (Sawchenko et al., 1984; Whitnall et al., 1985; Simmons and Swanson, 2009; Biag et al., 2011). In contrast, in the zebrafish NPO, many neuropeptides produced by tightly packed cells are not coexpressed, though some combinations show varying levels of coexpression, from occasional to moderate (Herget and Ryu, 2015). Assuming that the expression and coexpression profile of NPO cells can undergo stress-derived plasticity, as occurs with PVN cells (Kiss, 1988; Harbuz and Lightman, 1989; Swanson, 1991; Kurrasch et al., 2009), ELC may alter the degree of expression and coexpression of key NPO neuropeptides.

The expression profile of steroidogenic enzymes involved in glucocorticoid biosynthesis has been documented in developing zebrafish (Weger et al., 2018). Cortisol biosynthesis in zebrafish involves contributors such as *hsd11b2* (11-hydroxysteroid dehydrogenase type 2), crucial for cortisol inactivation (Krozowski, 1999; Alderman and Vijayan, 2012; Theodoridi et al., 2021); *cyp11c1* (11β-hydroxylase), essential for the synthesis of 11-ketotestosterone and cortisol (Tokarz et al., 2015; Nelson et al., 2013); and *star* (steroidogenic acute regulatory protein), responsible for cholesterol transport (Stocco, 2000). Studies in fish have reported a correlation between whole-body cortisol levels and the expression of *hsd11b2* and *cyp11c1* (Tsalafouta et al., 2014). Prolonged cortisol release has been observed in stressed zebrafish lacking functional Hsd11b2 (Theodoridi et al., 2021). Transgenic zebrafish larvae expressing Beggiatoa photoactivated adenylyl cyclase (bPAC) under a StAR promoter (Ryu et al., 2010; Stierl et al., 2011) have achieved light-dependent enhancement of steroidogenic cell activity in the interrenal gland, thereby elevating cortisol levels (Gutierrez-Triana et al., 2015). This approach can also be used to induce sustained hypercortisolemia (Nagpal et al., 2022). ELC may alter the expression of these genes involved in cortisol synthesis, as well as those responsible for and sensitive to HPI axis activation and GR signalling. These genes include *crh*, *avp* (arginine vasopressin), *oxt* (oxytocin), *crhr1* (corticotropin-releasing hormone receptor 1), the ACTH precursor *pomca* (pro-opiomelanocortin), *mc2r* (adrenocorticotropic hormone receptor), *nr3c2* (mineralocorticoid receptor, MR), *nr3c1* (glucocorticoid receptor, GR), and the stress-responsive GR-regulator *fkbp5* (FK506 binding protein 5) (Sinars et al., 2003; Zannas et al., 2016; Hartmann et al., 2021).

Additionally, we recently examined whole-body cortisol dynamics in 6 dpf larvae subjected to a 3-minute vortex. Cortisol levels were elevated 10 minutes after the vortex and returned to baseline within 30-40 minutes, depending on the vortex's intensity. After a second vortex, cortisol levels rose above baseline when administered 60 or 120 minutes after the first

vortex, but not after 30 minutes. Treatment with a GR blocker delayed the return to baseline and suppressed this refractory period, indicating GR-dependent early-phase feedback regulation (Castillo-Ramírez et al., 2024). The post-ELC cortisol response of larvae to a second vortex shortly after the first, especially within the 30-minute refractory period, is unknown. Addressing this question can provide insights into the effects of ELC on a larva's capacity for cortisol regulation during repeated stress.

Here, we characterize features of the HPI axis and cortisol response in zebrafish larvae following ELC induced by vortex flows. First, we examined how ELC in the form of sustained involuntary swimming at 5 dpf affects cortisol response dynamics following a 3-minute vortex at 6 dpf. We then examined how ELC impacts the expression and co-expression of *crh*, *avp*, and *oxt* in the larval NPO. Focusing on these peptides is justified by their established roles in mammals and their conserved functions in stress response and homeostasis in zebrafish. CRH initiates the body's response to stress and influences autonomic and behavioural responses; AVP plays a crucial role in stress response, social behaviour, and cardiovascular functions, including osmoregulation and blood pressure regulation; and OXT is known for its role in modulating stress and anxiety, social bonding, and reproductive behaviour (Swanson and Sawchenko, 1983; Herman and Cullinan, 1997; Eaton et al., 2008). Additionally, we explored the effect of ELC on the transcript levels of the previously listed genes involved in HPI axis activity, cortisol synthesis, cortisol inactivation, and GR signalling, under both baseline conditions and after vortex exposure. Lastly, we examined how ELC at 5 dpf modifies the cortisol response of 6 dpf larvae to a second vortex during the 30-minute refractory period following an initial vortex exposure. The results are discussed in the context of how ELC impacts cortisol responsiveness to stress and may influence HPI axis development, supporting the larval zebrafish as a model for studying developmental programming of stress axis function.

Results

Diminished glucocorticoid reactivity to initial stressor after prolonged stress axis activation. We first exposed 5 dpf larvae to either vortex flows for 9 hours (ELC larvae) or equal handling without vortex exposure (control larvae). At 6 dpf, we compared the basal whole-body cortisol levels (Fig. 1A) and the cortisol time course following a 3-minute vortex (Fig. 1B) between ELC and control larvae. Consistent with previous data (Castillo-Ramírez et al., 2019), both ELC and control larvae showed similar mean basal whole-body cortisol levels at 6 dpf. The 3-minute vortex transiently increased whole-cortisol in both groups, yet ELC larvae showed reduced GC_R to the vortex (Fig. 1C, D). Additionally, baseline whole-body cortisol levels in ELC larvae showed less variation (Fig. 1C). These results confirm that prolonged forced swimming at 5 dpf diminishes a larva's subsequent cortisol response to the first instance of homotypic stress. This likely results from adjustments in the state variables that control HPI axis reactivity, raising questions about how such changes relate to the expression and co-expression levels of neuropeptides in the NPO and how they may alter the NPO's capacity to influence downstream HPI axis activity.

NPO imaging reveals expression and coexpression of key neuropeptides correlated with early life challenge. We therefore explored whether the changes in cortisol response to the first instance of homotypic stress observed at 6 dpf in the ELC larvae (Fig. 1) are linked to alterations in the expression of *crh*, *avp*, and *oxt* in the larval NPO. For this, we implemented the ELC protocol at 5 dpf in conjunction with multicolor fluorescent *in situ* hybridization at 6 dpf (see Methods). We then compared the numbers of *crh*-, *avp*-, or *oxt*-positive cells in the NPO of unstressed subjects from both groups, ELC and control larvae. Quantification of cell numbers revealed that, compared to control larvae, ELC larvae had fewer *crh*-positive cells within the NPO, as well as fewer *oxt*-positive and fewer *avp*-positive cells (Fig. 2A), in line

with the idea that ELC can alter the expression of NPO neuropeptides. Additionally, we examined the degree of coexpression between sets of two neuropeptides in the same cell in ELC and control larvae using systematic cell by cell comparisons of pairwise combinatorial ISH staining of *avp*, *crh*, and *oxt* in the larval NPO (Fig. 2B, C). In both groups, ELC and control larvae, coexpression was consistently high for the combination of *avp* and *crh*, low or moderate for the *crh* and *oxt* combination, and absent or rare for the *oxt* and *avp* combination, in line with previous data (Herget and Ryu, 2015). Also, coexpression was consistently lower in ELC larvae for the combination *avp* and *crh* staining compared to control larvae (Fig. 2B). These results indicate that the changes in GC_R observed at 6 dpf in ELC larvae correlate with altered levels of both the expression and coexpression of *avp*, *crh*, and *oxt* in the larval NPO.

Early life challenge correlates with changes in the transcript abundance of genes involved in cortisol response and homeostasis. Next, we explored whether ELC at 5 dpf correlates with changes in the transcript levels of *hsd11b2*, *cyp11c1*, *star*, *crh*, *avp*, *oxt*, *crhr1*, *pomca*, *mc2r*, *nr3c2*, *nr3c1*, and *fkbp5* at 6 dpf, under both baseline conditions and after a 3-minute vortex. These genes play roles in cortisol synthesis, HPI axis activation, cortisol inactivation, and GR signalling. We employed RT-qPCR to quantify total RNAs from both ELC and control larvae, measuring the fold change in transcript abundance of the 12 genes (Table 1) relative to reference samples from control larvae. Samples were taken at baseline and at 30, 60, and 120 minutes after exposure to the 3-minute vortex (see Methods). The results indicated that ELC at 5 dpf led to altered expression of ten out of the twelve genes by 6 dpf (Fig. 3). Compared to controls, ELC larvae showed higher expression of *hsd11b2* under both baseline and stress conditions. Following the 3-minute vortex, ELC larvae also showed elevated expression of *cyp11c1*, *star*, *crh*, *oxt*, *crhr1*, *pomca*, *nr3c2*, *nr3c1*, and *fkbp5*. Furthermore, in ELC larvae, transcript levels of *nr3c2*, *mc2r*, and *crhr1* increased progressively following the vortex, whereas *fkbp5* transcript levels initially rose and later

declined post-vortex in both ELC and control larvae (Fig. 3A-L). We measured total RNA from ELC and control larvae without isolating expression profiles specifically within the NPO, pituitary, or interrenal gland. Consequently, whole-body qPCR cannot exclusively reflect changes in transcript levels within the HPI axis. Some of the selected genes are ubiquitously expressed, while others have more restricted expression, although still extending beyond the HPI axis. Nevertheless, the overall transcript abundance pattern observed in ELC larvae (Fig. 3M) suggests enhanced cortisol inactivation under both baseline and stress conditions, along with an increased capacity for cortisol synthesis and availability of stress modulators upon stress initiation.

Early life challenge alters glucocorticoid reactivity to a second vortex during the refractory period after the first vortex. A diminished capacity of the NPO to influence HPI axis reactivity, combined with enhanced cortisol inactivation resulting from ELC, may partly explain the reduced GC_R observed after the initial post-ELC vortex. Additionally, increased cortisol synthesis capacity and availability of stress modulators could impact GC_R dynamics during subsequent homotypic stress events, potentially affecting responses to a second vortex. To explore this, at 6 dpf, we compared whole-body cortisol levels in ELC and control larvae following two consecutive 3-minute vortices applied within the 30-minute refractory period after the initial exposure (Castillo-Ramírez et al., 2024) (Fig. 4A). ELC larvae showed increased whole-body cortisol in response to the second vortex applied during this refractory period, whereas control larvae did not (Fig. 4B). Both ELC and control larvae had similar baseline cortisol levels (Fig. 4C, see also Fig. 1C). However, ELC larvae showed comparable cortisol responses to both the first and second vortices (Fig. 4D), with their GC_R to the second vortex being 91% of the response to the first vortex, compared to 18% in control larvae (Fig. 4E). These results suggest that prolonged forced swimming at 5 dpf enhances a larva's ability

at 6 dpf to regulate cortisol levels and adjust HPI axis activity in response to environmental demands, thereby improving their coping with homotypic stress.

Discussion

Here we provide strong evidence for extended effects of early forced swimming on cortisol regulation and stress responsiveness in zebrafish larvae. We observed that ELC at 5 dpf resulted in significant alterations in cortisol reactivity to subsequent stress events. Specifically, ELC larvae had similar baseline cortisol levels compared to controls but showed reduced GC_R to a single vortex at 6 dpf. This finding is consistent with previous data (Castillo-Ramírez et al., 2019) and reveals adaptive adjustments in stress axis function following prolonged early-life stressor exposure. Notably, while ELC larvae showed reduced GC_R to the initial stressor, they had increased cortisol responsiveness to a second stress event occurring within the 30-minute refractory period following the first vortex (Castillo-Ramírez et al., 2024). This dual response pattern suggests that ELC larvae have enhanced stress responsiveness during homotypic stress, potentially due to adaptive changes in HPI axis signalling and cortisol metabolism.

Our findings are consistent with research in fish and other vertebrates showing that early life stress and GC manipulation can have lasting effects on HPA/I axis function and stress responsiveness. In larval zebrafish, optogenetic techniques enable non-invasive control of endogenous GC levels (De Marco et al., 2013; 2016). Transgenic larvae expressing Beggiatoa photoactivated adenylyl cyclase (bPAC) (Ryu et al., 2010; Stierl et al., 2011) under a StAR promoter can induce light-dependent activation of interrenal gland steroidogenic cells, resulting in elevated cortisol levels (Gutierrez-Triana et al., 2015). Persistent activation of these cells during early development leads to chronically high cortisol levels and a diminished cortisol response to later stressors (Nagpal et al., 2024). Additionally, optogenetically

elevated GC levels early in life disrupt hypothalamic neurogenesis, causing precocious development, failed maturation, and impaired feeding and growth (Eachus et al., 2024). Chronic stress induced by random shocks in developing zebrafish also causes sustained high cortisol levels and increased expression of glucocorticoid and mineralocorticoid receptors, which correlate with increased anxiety-like behaviour and elevated cortisol levels later in life (Chin et al., 2022). Zebrafish exposed to air-exposure stress at different developmental stages showed increased cortisol levels, altered stress responses, and changes in ion concentrations (Hare et al., 2021). Similar trends are observed in other species. In rainbow trout, chronic cortisol intake and daily stress exposure reduce GC_R (Barton et al., 1987). Rodent studies show that neonatal rats treated with dexamethasone show reduced GC_R in response to cold and restraint stress later in life (Felszeghy et al., 2000), while mice subjected to prolonged low-dose corticosterone exposure show suppressed GC_R, adrenal atrophy, and decreased CRH mRNA levels in the PVN (Kinlein et al., 2015). In humans, infants exposed to high cortisol levels in utero show elevated baseline cortisol and reduced GC_R in response to separation stress (O'Connor et al., 2013). Collectively, these observations underscore the complex interplay between ELC, GC regulation, and stress responsiveness early in life. However, the mechanisms through which ELC affects HPA/I axis function and leads to long-term changes in stress response patterns are still largely unclear, particularly regarding the initial phase of this interaction.

ELC larvae had fewer *crh*-, *avp*-, and *oxt*-positive NPO cells compared to controls, and the co-expression of *crh* and *avp* was diminished. These findings suggest that ELC acts on the adaptive plasticity in neuropeptide expression of the developing NPO, potentially affecting downstream HPI axis activity. The reduced count of *crh*- and *avp*-positive NPO cells in ELC larvae may contribute to their diminished GC_R to the initial vortex. These observations support the notion that the NPO serves as a neuronal locus for GC feedback, due to its homology to the mammalian PVN (Ziv et al., 2012; Herget et al., 2014; Facchinello et

al., 2017). Whole body qPCR revealed upregulation of *hsd11b2* in ELC larvae under both baseline and stress conditions, as well as upregulation of *cyp11c1*, *star*, *crh*, *oxt*, *crhr1*, *pomca*, *nr3c2*, *nr3c1*, and *fkbp5* following a 3-minute vortex, consistent with previous findings (Alsop and Vijayan, 2008). Interestingly, ELC larvae had fewer NPO *crh*-positive cells but showed increased whole-body *crh* upon acute stress. Further exploration should focus on the impact of ELC on the maturation of stress-related circuits involving NPO *crh*-positive cells (Bolton et al., 2022). Additionally, in ELC larvae, transcript levels of *nr3c2*, *mc2r*, and *crhr1* increased progressively post-vortex. Although limited by a lack of HPI axis specificity, these observations collectively suggest that ELC at 5 dpf can lead to altered expression of genes involved in cortisol metabolism, stress responsiveness, and GR signalling by 6 dpf. Studies in fish have reported a correlation between whole-body cortisol and mRNA levels of *hsd11b2* and *cyp11c1* (Tsalafouta et al., 2014). Also, prolonged cortisol release has been observed in stressed zebrafish lacking functional Hsd11b2 (Theodoridi et al., 2021). Overall, the observed expression and co-expression patterns of *avp*, *crh*, and *oxt* in the NPO, combined with transcript data, suggest that ELC enhances cortisol regulation. This could help prevent excess cortisol release and ensure an appropriate response to homotypic stress (Fig. 5).

Our findings contribute to understanding how early environments shape subsequent GC_R, NPO plasticity, and GC pathways during the early stages of HPI axis development. They highlight the value of the larval zebrafish as a model organism for studying the developmental programming of HPI axis function (de Abreu et al., 2021; Eachus et al., 2021; Swaminathan et al., 2023; Weinstock, 2008; Glover et al., 2010; Moisiadis and Matthews, 2014). Future research should explore the effects of early-life conditions on cortisol production in interrenal cells (Wilson et al., 2016) and the maturation of stress-related circuits in the NPO.

Methods

Zebrafish husbandry and handling

Zebrafish breeding and maintenance were performed under standard conditions (Westerfield, 2000). Groups of thirty wild-type embryos (cross of AB and TL strains, AB/TL) were collected in the morning and raised on a 12:12 light/dark cycle at 28 °C in 35 mm Petri dishes with 5 ml of E2 medium. At 3 dpf, the E2 medium was renewed, and chorions and debris were removed from the dishes. Experiments were carried out with 5-6 dpf larvae. Zebrafish experimental procedures were performed according to the guidelines of the German animal welfare law and approved by the local government (Regierungspräsidium Karlsruhe; G-29/12).

Water vortex flows

We used water vortex flows in a high-throughput fashion to induce rheotaxis and cortisol increase. Groups of thirty (either 5 or 6 dpf) larvae in 35 mm Petri dishes with 5 ml of E2 medium were exposed to vortex flows caused by the spinning movements of small magnetic stir bars (6 x 3mm, Fisherbrand, #11888882, Fisher scientific, Leicestershire, UK) inside the dishes. The Petri dishes, each with a single stir bar, were positioned on magnetic stirrer plates (Variomag, Poly 15; Thermo Fisher Scientific, Leicestershire, UK) and kept at 28°C inside an incubator (RuMed 3101, Rubarth Apparate GmbH, Laatzen, Germany). Larvae were exposed to either short (3 minutes, applied only to 6 dpf larvae) or long (9 hours of continuous stimulation, applied only to 5 dpf larvae) periods of vortex flows generated by a stirrer plate set at 330 revolutions per minute (rpm). This setting aimed to avoid ceiling effects caused by maximum levels of vortex-induced cortisol increase (Castillo-Ramírez et al., 2019). Previous studies have confirmed that the magnetic field inversions of the stirrer plate do not alter whole-body cortisol levels in larval zebrafish (Castillo-Ramírez et al., 2019). The prolonged

9-hour exposure at 5 dpf was designed to maximize exposure time within the constraints of the light/dark cycle. Control larvae underwent identical handling procedures without exposure to vortex flows (i.e., Petri dishes lacked stir bars). After vortex exposure, 6 dpf larvae were immobilized in ice water for subsequent cortisol detection or total RNA extraction (details below). Basal cortisol levels were measured before the initial exposure to vortex flows.

Re-exposure to vortex flows

At 6 dpf, subjects that had or had not been exposed to a 9-h period of forced swimming at 5 dpf (ELC and control larvae, respectively) underwent a 3-minute forced swimming session either once (Figs. 1, Fig. 3) or twice (Fig. 4), with the second exposure occurring 30 minutes after the first. Subsequently, larvae were used for cortisol detection, RNA extraction, or whole-mount fluorescent *in situ* hybridization and immunohistochemistry (see below). Basal levels of cortisol, RNA, cell number and coexpression in 6 dpf larvae were measured before their initial exposure to vortex flows.

Whole-body cortisol

The procedures and the home-made ELISA used for cortisol measurements were as described previously (Yeh et al., 2013). After exposure to the vortex, groups of thirty larvae were immobilized in ice water. Unexposed larvae were collected after equal handling, omitting stressor exposure. The samples were then frozen in an ethanol/dry-ice bath and stored at −20 °C for subsequent extraction. Each replicate consisted of a well with 30 larvae. Cortisol extraction and detection were carried out between 10:30 and 11:30 hours.

qPCR

Like cortisol, total RNA was extracted from groups of thirty larvae. Isolation of total RNA was performed using the RNeasy Micro Kit (Qiagen, Hilden, Germany). Quantitation and quality

control of isolated RNA was evaluated by running a chip (RNA6000 Pico Kit, Agilent Technologies, Santa Clara, CA, USA) on a bioanalyzer (Agilent 2100, Agilent Technologies, Santa Clara, CA, USA). RNA was then used as template for real time qPCR using the Power SYBR Green RNA-to-Ct 1 Step Kit (Thermo Fisher Scientific, Leicestershire, UK). Primer sequences (Table 1) were obtained from literature and GETPrime (Swiss Federal Institute of Technology, Lausanne, Switzerland) (David et al., 2017). All primers were tested for efficiency by running serial dilutions of samples. Efficiency (E) was defined as $E=10^{(-1/slope)^{-1}}$, with *slope* calculated from the template concentration (log) vs Ct value curve. Only primers with a 100 % (± 10 %) efficiency were considered for further experiments. Real time qPCR was carried out in a 7500 Real Time PCR system (Applied Biosystems, Waltham, MA, USA) and data was analyzed using the $2^{-\Delta\Delta Ct}$ method to calculate relative gene expression (Livak and Schmittgen, 2001).

Whole-mount fluorescent in situ hybridization, immunohistochemistry, and imaging

Whole-mount fluorescent *in situ* hybridization and immunohistochemistry were performed as described elsewhere (Kastenhuber et al., 2010; Lauter et al. 2011), using riboprobes for *avp* (Eaton et al., 2008), *oxt* (Unger and Glasgow, 2003), and *crh* (Löhr et al., 2009), and a primary chicken antibody labeling GFP (1:500, Abcam), with a secondary anti-chicken Alexa 488 antibody (1:1000, invitrogen). For imaging, specimens were cleared in 80% glycerol (Gerbu) in PBS for 1 h. Confocal stacks were recorded using a Leica SP5 confocal microscope with a Nikon 20x glycerol objective. Each channel was recorded sequentially to reduce interfering signals from overlapping emission spectra. Zoom, dimensions, gain, offset, average, and speed were adjusted for each stack to obtain the optimal image quality of the desired volume. Stacks were evaluated using Amira 5.4 (Thermo Fisher Scientific, Leicestershire, UK) to create maximum intensity projections, which were spatially restricted

to the volume of interest, excluding signals from planes in front or behind. Brightness and contrast were adjusted for each channel.

Independent sampling

Cortisol, cell counting, and RT-qPCR measurements were conducted on distinct groups of larvae, all subjected to the same treatment, ensuring fully independent samples. In every instance, measurements were taken from larvae housed in wells containing a total of thirty individuals. Consequently, the larval density per well remained a constant factor during vortex flow exposure, preventing any confounding effects. For the cell counting measurements, each replicate involved a single larva. For cortisol and RT-qPCR measurements, all thirty larvae within a well were utilized. Each replication was entirely independent from the others, thus avoiding pseudo-replication.

General experimental design and statistical analyses

We employed a between-groups design in all experiments. Treatments were randomly assigned to replicates. Blinding was implemented. For measurements of cortisol, cell counting, and RT-qPCR, a first experimenter conducted treatments, collected samples, and applied initial labels. A second experimenter performed measurements on the labelled samples and subsequently assigned them new labels. The first experimenter then quantified cortisol levels, cell numbers, or gene expression using the newly labelled samples. All data are shown as box and whiskers (min to max) including all data points (Fig. 1C, Fig. 3A-L, Fig. 4C-E), box and whiskers (min to max) (Fig. 4B), mean and standard error of the mean (Fig. 1D), or single measurement points (plus median, Fig. 2A, C). No data points or samples were excluded from analysis. Statistical methods to predetermine sample size were not necessary. Our sample sizes are similar to (or larger than) those generally employed in the field, and based on previous publications (Yeh et al., 2013; Castillo-Ramírez et al., 2019; De

Marco et al., 2016). Data were tested for normality and homoscedasticity using the Shapiro-Wilk and KS normality tests and the Brown–Forsythe and Bartlett's tests, respectively. In Fig. 1C, due to non-normality and lack of homoscedasticity, we used the Mann-Whitney test. In Fig. 1D, we applied Kruskal-Wallis tests to accommodate datasets lacking homoscedasticity across time, followed by unpaired two-tailed t-tests for comparisons meeting normality and homoscedasticity. In Fig. 2A and Fig. 2C, where normality and homoscedasticity were not met, we used Mann-Whitney tests. In Fig. 3, we used Kruskal-Wallis tests due to non-normality and lack of homoscedasticity, assessing time effects, followed by two-group comparisons using unpaired two-tailed t-tests or Mann-Whitney tests. In Fig. 4B-E, we used unpaired two-tailed t-tests and one-sample t-tests against a fold change of '1'. Statistical analyses were performed using MS-Excel (Microsoft Corp; Redmond, WA, USA) and Prism 10.2.0 (Graphpad Software Inc, San Diego, CA, USA).

Data availability

The experimental datasets presented in this study are available in online repositories, accessible upon request from the authors.

Ethics

The present study was reviewed and approved by Regierungspräsidium Karlsruhe; G-29/12.

Funding

This work was supported by the Max Planck Society, the University Medical Center of the Johannes Gutenberg University Mainz, and Liverpool John Moores University.

Author Contributions

Luis A. Castillo-Ramírez, Conceptualization, Data curation, Formal analysis, Investigation, Validation, Methodology, Writing - original draft; Ulrich Herget, Data curation, Formal analysis, Methodology, Writing – original draft; Soojin Ryu, Conceptualization, Resources, Supervision, Funding acquisition, Methodology, Project administration, Writing – review; Rodrigo J. De Marco, Conceptualization, Resources, Supervision, Funding acquisition, Investigation, Validation, Methodology, Data curation, Formal analysis, Visualization, Project administration, Writing - original draft, Writing - review and editing.

Acknowledgments

We would like to thank L. Flores-García for assistance with the experiments, Karl J. Iremonger and Chrysanthi Fergani for providing useful comments on a previous draft, R. Singer and A. Schoell for expert fish care, and R. Rödel for technical support.

Competing Interests

The authors declare that the research was conducted in the absence of any commercial or financial relationships that could be construed as a potential conflict of interest.

References

Alderman, S.L. and Bernier, N.J. (2009). Ontogeny of the corticotropin-releasing factor system in zebrafish. *Gen. Comp. Endocrinol.* **164**(1),61-9. doi: 10.1016/j.ygcen.2009.04.007.

Alderman, S.L. and Vijayan, M.M. (2012). 11β-Hydroxysteroid dehydrogenase type 2 in zebrafish brain: a functional role in hypothalamus-pituitary-interrenal axis regulation. *J. Endocrinol.* **215**(3),393-402. doi: 10.1530/JOE-12-0379.

Alsop, D. and Vijayan, M.M. (2008). Development of the corticosteroid stress axis and receptor expression in zebrafish. *Am. J. Physiol. Regul. Integr. Comp. Physiol.* **294**(3),R711-9. doi.org/10.1152/ajpregu.00671.2007

Alsop, D. and Vijayan, M.M. (2009). Molecular programming of the corticosteroid stress axis during zebrafish development. *Comp. Biochem. Physiol. A. Mol. Integr. Physiol.* **153**(1),49-54. doi.org/10.1016/j.cbpa.2008.12.008

Barton, B.A., Schreck, C.B. and Barton, L.D. (1987). Effects of chronic cortisol administration and daily acute stress on growth, physiological conditions, and stress responses in juvenile rainbow trout. *Dis. Aquat. Org.* **2**,173–185. doi:10.3354/DAO002173.

Biag, J., Huang, Y., Gou, L., Hintiryan, H., Askarinam, A., Hahn, J.D., Toga, A.W., and Dong, H.W. (2012). Cyto- and chemoarchitecture of the hypothalamic paraventricular nucleus in the C57BL/6J male mouse: a study of immunostaining and multiple fluorescent tract tracing. *J. Comp. Neurol.* **520**(1),6-33. doi: 10.1002/cne.22698.

Biran, J., Tahor, M., Wircer, E. and Levkowitz, G. (2015). Role of developmental factors in hypothalamic function. *Front. Neuroanat.* **9**,47. doi: 10.3389/fnana.2015.00047.

Bolton, J.L., Short, A.K., Othy, S., Kooiker, C.L., Shao, M., Gunn, B.G., Beck, J., Bai, X., Law, S.M., Savage, J.C., et al. (2022). Early stress-induced impaired microglial pruning of excitatory synapses on immature CRH-expressing neurons provokes aberrant adult stress responses. *Cell Rep.* **38**(13),110600. doi: 10.1016/j.celrep.2022.110600.

Castillo-Ramírez, L.A., Ryu, S., and De Marco, R.J. (2019). Active behaviour during early development shapes glucocorticoid reactivity. *Sci. Rep.* **9**(1),12796. doi: 10.1038/s41598-019-49388-3.

Castillo-Ramírez, L.A., Ryu, S., and De Marco, R.J. (2024). Cortisol dynamics and GR-dependent feedback regulation in zebrafish larvae exposed to repeated stress. bioRxiv doi: https://doi.org/10.1101/2024.08.07.606983

Champagne, D.L., and Richardson, M.K. (2013). Patterns of cortisol reactivity to stress and the development of coping style in zebrafish *Danio rerio*. *J. Neuroendocrinol.* **25**(9),750-61. doi: 10.1111/jne.12053.

Charmandari, E., Tsigos, C., and Chrousos, G. (2005). Endocrinology of the stress response. *Annu. Rev. Physiol.* **67**,259-84. doi: 10.1146/annurev.physiol.67.040403.120816.

Chin, J.S.R., Phan, T.N., Albert, L.T., Keene, A.C., and Duboué, E.R. (2022). Long lasting anxiety following early life stress is dependent on glucocorticoid signaling in zebrafish. *Sci. Rep.* **12**(1),12826. doi: 10.1038/s41598-022-16257-5.

Chrousos, G.P. (1998). Stressors, stress, and neuroendocrine integration of the adaptive response. The 1997 Hans Selye Memorial Lecture. *Ann. N. Y. Acad. Sci.* **851**,311-35. doi: 10.1111/j.1749-6632.1998.tb09006.x.

Dallman, M.F. (2005). Fast glucocorticoid actions on brain: Back to the future. *Front. Neuroendocrinol.* **26**(3-4),103-8. doi: 10.1016/j.yfrne.2005.08.001.

Dallman, M.F., and Yates, F.E. (1969). Dynamic asymmetries in the corticosteroid feedback path and distribution-metabolism-binding elements of the adrenocortical system. *Ann. N. Y. Acad. Sci*. **156**(2),696-721. doi: 10.1111/j.1749-6632.1969.tb14008.x.

Dallman, M.F., Akana, S.F., Levin, N., Walker, C.D., Bradbury, M.J., Suemaru, S., and Scribner, K.S. (1994). Corticosteroids and the control of function in the hypothalamo-pituitary-adrenal (HPA) axis. *Ann. N. Y. Acad. Sci.* **746**,22-31. doi: 10.1111/j.1749-6632.1994.tb39206.x.

David, F.P., Rougemont, J., and Deplancke, B. (2017). GETPrime 2.0: gene- and transcript-specific qPCR primers for 13 species including polymorphisms. *Nucleic Acids Res.* **45**(D1),D56-D60. doi: 10.1093/nar/gkw913.

de Abreu, M.S., Demin, K.A., Giacomini, A.C.V.V., Amstislavskaya, T.G., Strekalova, T., Maslov, G.O., Kositsin, Y., Petersen, E.V., and Kalueff, A.V. (2021). Understanding

how stress responses and stress-related behaviors have evolved in zebrafish and mammals. *Neurobiol. Stress.* **15**,100405. doi: 10.1016/j.ynstr.2021.100405.

de Kloet, E.R., and Joëls, M. (2023). The cortisol switch between vulnerability and resilience. *Mol. Psychiatry* **29**(1),20-34. doi: 10.1038/s41380-022-01934-8.

de Kloet, E.R., Vreugdenhil, E., Oitzl, M.S., and Joëls, M. (1998). Brain corticosteroid receptor balance in health and disease. *Endocr. Rev.* **19**(3),269-301. doi: 10.1210/edrv.19.3.0331.

De Marco, R.J., Groneberg, A.H., Yeh, C.M., Castillo-Ramírez, L.A., and Ryu, S. (2013). Optogenetic elevation of endogenous glucocorticoid level in larval zebrafish. *Front. Neural Circuits* **7**,82. doi: 10.3389/fncir.2013.00082.

De Marco, R.J., Thiemann, T., Groneberg, A.H., Herget, U., and Ryu, S. (2016). Optogenetically enhanced pituitary corticotroph cell activity post-stress onset causes rapid organizing effects on behaviour. *Nat. Commun.* **7**,12620. doi: 10.1038/ncomms12620

Eachus, H., Choi, M.K., and Ryu, S. (2021). The Effects of Early Life Stress on the Brain and Behaviour: Insights From Zebrafish Models. *Front. Cell Dev. Biol.* **9**,657591. doi: 10.3389/fcell.2021.657591.

Eachus, H., Choi, M.K., Tochwin, A., Kaspareit, J., Ho, M., and Ryu, S. (2024). Elevated glucocorticoid alters the developmental dynamics of hypothalamic neurogenesis in zebrafish. *Commun. Biol.* **7**(1),416. doi: 10.1038/s42003-024-06060-5.

Eaton, J.L., Holmqvist, B., and Glasgow, E. (2008). Ontogeny of vasotocin-expressing cells in zebrafish: selective requirement for the transcriptional regulators orthopedia and single-minded 1 in the preoptic area. *Dev. Dyn.* **237**(4),995-1005. doi: 10.1002/dvdy.21503.

Egan, R.J., Bergner, C.L., Hart, P.C., Cachat, J.M., Canavello, P.R., Elegante, M.F., Elkhayat, S.I., Bartels, B.K., Tien, A.K., Tien, D.H., et al. (2009). Understanding behavioral and physiological phenotypes of stress and anxiety in zebrafish. *Behav. Brain Res.* **205**(1),38-44. doi: 10.1016/j.bbr.2009.06.022.

Facchinello, N., Skobo, T., Meneghetti, G., Colletti, E., Dinarello A, Tiso N, Costa R, Gioacchini G, Carnevali O, Argenton F, et al. (2017). nr3c1 null mutant zebrafish are viable and reveal DNA-binding-independent activities of the glucocorticoid receptor. *Sci. Rep.* **7**(1),4371. doi: 10.1038/s41598-017-04535-6.

Felszeghy, K., Bagdy, G., and Nyakas, C. (2000). Blunted pituitary-adrenocortical stress response in adult rats following neonatal dexamethasone treatment. *J. Neuroendocrinol.* **12**(10),1014-21. doi: 10.1046/j.1365-2826.2000.00551.x.

Glover, V., O'Connor, T.G., and O'Donnell, K. (2010). Prenatal stress and the programming of the HPA axis. *Neurosci. Biobehav. Rev.* **35**(1),17-22. doi: 10.1016/j.neubiorev.2009.11.008.

Gutierrez-Triana, J.A., Herget, U., Castillo-Ramírez, L.A., Lutz, M., Yeh, C.M., De Marco, R.J., and Ryu. S. (2015). Manipulation of Interrenal Cell Function in Developing Zebrafish Using Genetically Targeted Ablation and an Optogenetic Tool. *Endocrinology* **156**(9),3394-401. doi: 10.1210/EN.2015-1021.

Hare, A.J., Zimmer, A.M., LePabic, R., Morgan, A.L., and Gilmour, K.M. (2021). Early-life stress influences ion balance in developing zebrafish (*Danio rerio*). *J. Comp. Physiol. B.* **191**(1):69-84. doi: 10.1007/s00360-020-01319-9.

Harbuz, M.S., and Lightman, S.L. (1989). Responses of hypothalamic and pituitary mRNA to physical and psychological stress in the rat. *J. Endocrinol.* **122**(3),705-11. doi: 10.1677/joe.0.1220705.

Hartmann, J., Bajaj, T., Klengel, C., Chatzinakos, C., Ebert, T., Dedic, N., McCullough, K.M., Lardenoije, R., Joëls, M., Meijer, O.C., et al. (2021). Mineralocorticoid receptors dampen glucocorticoid receptor sensitivity to stress via regulation of FKBP5. *Cell Rep.* **35**(9),109185. doi: 10.1016/j.celrep.2021.109185.

Herget, U., and Ryu, S. (2015). Coexpression analysis of nine neuropeptides in the neurosecretory preoptic area of larval zebrafish. *Front. Neuroanat.* **9**,2. doi: 10.3389/fnana.2015.00002.

Herget, U., Wolf, A., Wullimann, M.F., and Ryu, S. (2014). Molecular neuroanatomy and chemoarchitecture of the neurosecretory preoptic-hypothalamic area in zebrafish larvae. *J. Comp. Neurol.* **522**(7),1542-1564. doi: 10.1002/cne.23480.

Herman, J.P., and Cullinan, W.E. (1997). Neurocircuitry of stress: central control of the hypothalamo-pituitary-adrenocortical axis. *Trends Neurosci.* **20**(2),78-84. doi: 10.1016/s0166-2236(96)10069-2.

Kastenhuber, E., Kratochwil, C.F., Ryu, S., Schweitzer, J., and Driever, W. (2010). Genetic dissection of dopaminergic and noradrenergic contributions to catecholaminergic tracts in early larval zebrafish. *J. Comp. Neurol.* **518**(4),439-58. doi: 10.1002/cne.22214.

Kinlein, S.A., Wilson, C.D., and Karatsoreos, I.N. (2015). Dysregulated hypothalamic-pituitary-adrenal axis function contributes to altered endocrine and neurobehavioral responses to acute stress. *Front. Psychiatry.* **6**,31. doi: 10.3389/fpsyt.2015.00031.

Kiss, J.Z. (1988). Dynamism of chemoarchitecture in the hypothalamic paraventricular nucleus. *Brain Res. Bull.* **20**(6),699-708. doi: 10.1016/0361-9230(88)90080-9.

Krozowski, Z. (1999). The 11beta-hydroxysteroid dehydrogenases: functions and physiological effects. *Mol. Cell. Endocrinol.* **151**(1-2),121-7. doi: 10.1016/s0303-7207(98)00256-1.

Kurrasch, D.M., Nevin, L.M., Wong, J.S., Baier, H., and Ingraham, H.A. (2009). Neuroendocrine transcriptional programs adapt dynamically to the supply and demand for neuropeptides as revealed in NSF mutant zebrafish. *Neural Dev.* **4**,22. doi: 10.1186/1749-8104-4-22.

Lauter, G., Söll, I., and Hauptmann, G. (2011). Multicolor fluorescent in situ hybridization to define abutting and overlapping gene expression in the embryonic zebrafish brain. *Neural Dev.* **6**,10. doi: 10.1186/1749-8104-6-10.

Livak, K.J., and Schmittgen, T.D. (2001). Analysis of relative gene expression data using real-time quantitative PCR and the 2(-Delta Delta C(T)) Method. *Methods* **25**(4),402-8. doi: 10.1006/meth.2001.1262.

Löhr, H., Ryu, S., and Driever, W. (2009). Zebrafish diencephalic A11-related dopaminergic neurons share a conserved transcriptional network with neuroendocrine cell lineages. *Development* **136**(6),1007-17. doi: 10.1242/dev.033878.

Malkoski, S.P., and Dorin, R.I. (1999). Composite glucocorticoid regulation at a functionally defined negative glucocorticoid response element of the human corticotropin-releasing hormone gene. *Mol. Endocrinol.* **13**(10),1629-44. doi: 10.1210/mend.13.10.0351.

McEwen, B.S. (2007). Physiology and neurobiology of stress and adaptation: central role of the brain. *Physiol. Rev.* **87**(3),873-904. doi: 10.1152/physrev.00041.2006.

Moisiadis, V.G., and Matthews, S.G. (2014). Glucocorticoids and fetal programming part 1: Outcomes. *Nat. Rev. Endocrinol.* **10**(7),391-402. doi: 10.1038/nrendo.2014.73.

Munck, A., Guyre, P.M., and Holbrook, N.J. (1984). Physiological functions of glucocorticoids in stress and their relation to pharmacological actions. *Endocr. Rev.* **5**(1),25-44. doi: 10.1210/edrv-5-1-25.

Nagpal, J., Eachus, H., Lityagina, O., and Ryu, S. (2024). Optogenetic induction of chronic glucocorticoid exposure in early-life leads to blunted stress-response in larval zebrafish. *Eur. J. Neurosci.* **59**(11),3134-3146. doi: 10.1111/ejn.16301.

Nelson, D.R., Goldstone, J.V., and Stegeman, J.J. (2013). The cytochrome P450 genesis locus: the origin and evolution of animal cytochrome P450s. *Philos. Trans. R. Soc. Lond. B Biol. Sci*. **368**(1612),20120474. doi: 10.1098/rstb.2012.0474.

O'Connor, T.G., Bergman, K., Sarkar, P., and Glover, V. (2013). Prenatal cortisol exposure predicts infant cortisol response to acute stress. *Dev. Psychobiol.* **55**(2),145-55. doi: 10.1002/dev.21007.

Ryu, M.H., Moskvin, O.V., Siltberg-Liberles, J., and Gomelsky, M. (2010). Natural and engineered photoactivated nucleotidyl cyclases for optogenetic applications. *J. Biol. Chem.* **285**(53),41501-8. doi: 10.1074/jbc.M110.177600.

Sawchenko, P.E., Swanson, L.W., and Vale, W.W. (1984). Corticotropin-releasing factor: co-expression within distinct subsets of oxytocin-, vasopressin-, and neurotensin-immunoreactive neurons in the hypothalamus of the male rat. *J. Neurosci.* **4**(4),1118-29. doi: 10.1523/JNEUROSCI.04-04-01118.1984.

Shipston, M.J. (2022). Glucocorticoid action in the anterior pituitary gland: Insights from corticotroph physiology. *Curr. Opin. Endocr. Metab. Res.* **25**,100358. doi: 10.1016/j.coemr.2022.100358.

Simmons, D.M., and Swanson, L.W. (2009). Comparison of the spatial distribution of seven types of neuroendocrine neurons in the rat paraventricular nucleus: toward a global 3D model. *J. Comp. Neurol.* **516**(5),423-41. doi: 10.1002/cne.22126.

Sinars, C.R., Cheung-Flynn, J., Rimerman, R.A., Scammell, J.G., Smith, D.F., and Clardy, J. (2003). Structure of the large FK506-binding protein FKBP51, an Hsp90-binding protein and a component of steroid receptor complexes. *Proc. Natl. Acad. Sci. U. S. A.* **100**(3),868-73. doi: 10.1073/pnas.0231020100.

Stierl, M., Stumpf, P., Udwari, D., Gueta, R., Hagedorn, R., Losi, A., Gärtner, W., Petereit, L., Efetova, M., Schwarzel, M., et al. (2011). Light modulation of cellular cAMP by a small bacterial photoactivated adenylyl cyclase, bPAC, of the soil bacterium Beggiatoa. *J. Biol. Chem.* **286**(2),1181-8. doi: 10.1074/jbc.M110.185496.

Stocco, D.M. (2000). The role of the StAR protein in steroidogenesis: challenges for the future. *J. Endocrinol.* **164**(3),247-53. doi: 10.1677/joe.0.1640247.

Swaminathan, A., Gliksberg, M., Anbalagan, S., Wigoda, N., and Levkowitz, G. (2023). Stress resilience is established during development and is regulated by complement factors. *Cell Rep.* **42**(1),111973. doi: 10.1016/j.celrep.2022.111973.

Swanson, L.W. (1991). Biochemical switching in hypothalamic circuits mediating responses to stress. *Prog. Brain Res.* **87**,181-200. doi: 10.1016/s0079-6123(08)63052-6.

Swanson, L.W., and Sawchenko, P.E. (1983). Hypothalamic integration: organization of the paraventricular and supraoptic nuclei. *Annu. Rev. Neurosci.* **6**,269-324. doi: 10.1146/annurev.ne.06.030183.001413.

Tan, J.X.M., Ang, R.J.W., and Wee, C.L. (2022). Larval zebrafish as a model for mechanistic discovery in mental health. *Front. Mol. Neurosci.* **15**:900213. doi: 10.3389/fnmol.2022.900213.

Theodoridi, A., Dinarello, A., Badenetti, L., Pavlidis, M., Dalla Valle, L., and Tsalafouta, A. (2021). Knockout of the *hsd11b2* Gene Extends the Cortisol Stress Response in Both Zebrafish Larvae and Adults. *Int. J. Mol. Sci.* **22**(22):12525. doi: 10.3390/ijms222212525.

Tokarz, J., Möller, G., Hrabě de Angelis, M., and Adamski, J. (2015). Steroids in teleost fishes: A functional point of view. *Steroids* **103**,123-44. doi: 10.1016/j.steroids.2015.06.011.

Tsalafouta, A., Papandroulakis, N., Gorissen, M., Katharios, P., Flik, G., and Pavlidis, M. (2014). Ontogenesis of the HPI axis and molecular regulation of the cortisol stress response during early development in Dicentrarchus labrax. *Sci. Rep.* **4**,5525. doi: 10.1038/srep05525.

Unger, J.L., and Glasgow, E. (2003). Expression of isotocin-neurophysin mRNA in developing zebrafish. *Gene Expr. Patterns* **3**(1),105-8. doi: 10.1016/s1567-133x(02)00064-9.

Weger, M., Diotel, N., Weger, B.D., Beil, T., Zaucker, A., Eachus, H.L., Oakes, J.A., do Rego, J.L., Storbeck, K.H., Gut, P., et al. (2018). Expression and activity profiling of the

steroidogenic enzymes of glucocorticoid biosynthesis and the fdx1 co-factors in zebrafish. *J. Neuroendocrinol.* **30**(4),e12586. doi: 10.1111/jne.12586.

Weinstock, M. (2008). The long-term behavioural consequences of prenatal stress. *Neurosci. Biobehav. Rev.* **32**(6),1073-86. doi: 10.1016/j.neubiorev.2008.03.002.

Wendelaar Bonga, S.E. (1997). The stress response in fish. *Physiol. Rev.* **77**(3),591-625. doi: 10.1152/physrev.1997.77.3.591.

Westerfield, M. (2000). *The Zebrafish Book. A Guide for the Laboratory Use of Zebrafish (Danio rerio).* 4th ed. Eugene: Univ. of Oregon Press.

Whitnall, M.H., Mezey, E., and Gainer, H. (1985). Co-localization of corticotropin-releasing factor and vasopressin in median eminence neurosecretory vesicles. *Nature* **317**(6034),248-50. doi: 10.1038/317248a0.

Wilson, K.S., Tucker, C.S., Al-Dujaili, E.A., Holmes, M.C., Hadoke, P.W., Kenyon, C.J., and Denvir, M.A. (2016). Early-life glucocorticoids programme behaviour and metabolism in adulthood in zebrafish. *J. Endocrinol.* **230**(1),125-42. doi: 10.1530/JOE-15-0376.

Yeh, C.M., Glöck, M., and Ryu, S. (2013). An optimized whole-body cortisol quantification method for assessing stress levels in larval zebrafish. *PLoS One* **8**(11),e79406. doi: 10.1371/journal.pone.0079406.

Zannas, A.S., Wiechmann, T., Gassen, N.C., and Binder, E.B. (2016). Gene-Stress-Epigenetic Regulation of FKBP5: Clinical and Translational Implications. *Neuropsychopharmacology* **41**(1),261-74. doi: 10.1038/npp.2015.235.

Ziv, L., Muto, A., Schoonheim, P.J., Meijsing, S.H., Strasser, D., Ingraham, H.A., Schaaf, M.J., Yamamoto, K.R., and Baier, H. (2013). An affective disorder in zebrafish with mutation of the glucocorticoid receptor. *Mol. Psychiatry* **18**(6),681-91. doi: 10.1038/mp.2012.64.

Figure legends

Figure 1. Diminished glucocorticoid reactivity to initial stressor after prolonged stress axis activation. (**A**,**B**) Comparison steps for measuring: (**A**) baseline whole-body cortisol levels and (**B**) whole-body cortisol trajectory post-vortex in 6 dpf larvae with or without ELC exposure. (**C**,**D**) Baseline whole-body cortisol levels and whole-body cortisol trajectory post-vortex in control (black) and ELC (orange) larvae. (**C**) $p = 0.90$ (U = 17) by Mann-Whitney test; N per group = 6; box and whiskers (min to max), all data points shown. (**D**) Control: H = 27.0, $p < 0.0001$, ELC: H = 25.8, $p < 0.0001$ by Kruskal-Wallis tests; **$p < 0.01$ ($t_{(10)} = 3.2$), ***$p < 0.001$ ($t_{(10)} = 5.5$), ****$p < 0.0001$ ($t_{(10)} = 6.3$), 40': $p = 0.07$ ($t_{(10)} = 2.1$), 60': $p = 0.44$ ($t_{(10)} = 0.80$) by unpaired two-tailed *t*-tests; N per group = 6; Mean ± S.E.M. The red line represents the average baseline whole-body cortisol levels from (**C**).

Figure 2. Peptidergic NPO cell numbers in wildtype larvae with or without ELC exposure. (**A**) Comparison of cell numbers in the NPO with (orange; ELC larvae, N=20) or without (black; control larvae, N=27) ELC exposure. $p = 0.03$ (U = 167), $p = 0.0004$ (U = 112), $p < 0.0001$ (U = 85) by Mann-Whitney tests. (**B**) Maximum intensity projections of confocal stacks show NPO cells expressing *oxt* (green), *avp* (red), or *crh* (blue) in control (above) or ELC (below) larvae. Double-colour comparisons of each pairwise combination shown as well. Scale bar: 25 μm. (**C**) Comparison of coexpression levels in the NPO with (orange; ELC larvae, N = 20) or without (black; control larvae, N = 27) ELC stimulation. $p = 0.02$ (U = 787.5), $p = 0.002$ (U = 686), $p < 0.0001$ (U = 85) by Mann-Whitney tests. (**a**,**c**) All data points shown.

Figure 3. Transcript abundance of HPI axis signalling components in control and ELC larvae. (**A**-**L**) Fold change in the expression of HPI axis genes, relative to reference samples

from control subjects, assessed under both steady-state (basal) and stressed (30, 60, or 120 min after a high-strength vortex) conditions in both control (black) and ELC (orange) larvae; N per group = 5. H and p values from Kruskal-Wallis tests shown in black (control larvae) and orange (ELC larvae) in the top-left corners of each individual panel. Subsequent two-group comparisons were conducted using unpaired two-tailed *t*-tests or Mann-Whitney tests. (**B**,**C**,**E**,**F**,**G**,**H**,**J**) *$p < 0.05$, ****$p < 0.0001$ (**B**: $t_{(8)} = 2.9$; **C**: $t_{(8)} = 3.2$; **E**: $t_{(8)} = 2.5$; **F**: $t_{(8)} = 2.3$; **G**: $t_{(8)} = 7.3$; **H**: $t_{(8)} = 3.2$; **J**: $t_{(8)} = 3.2$). (**I**) *$p < 0.05$ (U = 1, 60'; $t_{(8)} = 3.1$, 120'). (**K**) **$p < 0.01$ (U = 0, 60', U = 0, 120'). (**L**) *$p < 0.05$, **$p < 0.01$ ($t_{(8)} = 2.6$, basal; U = 0, 30'; U = 0, 60'; U = 0, 120'). (**M**) Density grid summarising the comparison of fold change in the expression level of the 12 focal HPI axis genes relative to reference samples from control subjects under steady-state (basal) and stressed (30, 60, or 120 min after a single high-strength vortex) conditions in control and ELC larvae. N per group = 5. *p* values from Kruskal-Wallis tests are shown on the right side of the individual panels for both control and ELC larvae, followed by two-group comparisons using unpaired two-tailed *t*-tests or Mann-Whitney tests (*$p < 0.05$, **$p < 0.01$, ****$p < 0.0001$).

Figure 4. ELC alters GC_R to a second vortex during the refractory period after the first vortex. (**A**) Independent sampling for measuring GC_R to homotypic stress in 6 dpf larvae with or without ELC. (**B**) Whole-body cortisol following two 3-minute vortices applied within a 30-minute refractory period, during which 6 dpf larvae unexposed to ELC fail to show cortisol levels rising above baseline in response to a second 3-min vortex, in control (black) and ELC (orange) larvae. N per group = 6. ****$p < 0.0001$ ($t_{(10)} = 13.9$) by unpaired two-tailed *t*-test. (**C**) Baseline whole-body cortisol levels in ELC larvae relative to controls (data from **Fig. 1C**), depicted for the sake of interpreting panels (**D**) and (**E**); $p = 0.40$ ($t_{(5)} = 0.9$) by one-sample *t*-test against fold change of '1'. (**D**) GC_R to 1st and 2nd vortices relative to baseline in control and ELC larvae. Data from **Fig. 1C**, **Fig. 1D** (10 min post-vortex), and (**B**).

N per group = 6. ****$p < 0.0001$ (1st Control, $t_{(5)} = 17.4$, 1st ELC, $t_{(5)} = 21.4$, 2nd ELC, $t_{(5)} = 16.8$), $p = 0.23$ (2nd Control, $t_{(5)} = 1.4$) by one-sample *t*-tests against fold change of '1'; $p = 0.0003$ ($t_{(10)} = 5.4$), $p < 0.0001$ ($t_{(10)} = 14.5$) by unpaired two-tailed *t*-tests. (**E**) GC_R to the 2nd vortex relative to GC_R to the 1st vortex in control (black) and ELC (orange) larvae (data from **D**). *$p < 0.05$ ($t_{(5)} = 3.9$), ****$p < 0.0001$ ($t_{(5)} = 32.3$) by one-sample *t*-tests against fold change of '1'. $p < 0.0001$ ($t_{(10)} = 20.7$) by unpaired two-tailed *t*-test. (**B**-**E**) Box and whiskers (min to max), (**c**-**e**) all data points shown.

Figure 5. Proposed model illustrating the initial adaptation of the HPI axis following ELC. Prolonged early-life activation of the HPI axis, induced by increased environmental challenge, diminishes the NPO's capacity to influence downstream HPI axis activity. Baseline conditions show enhanced cortisol inactivation, which can persist upon stress onset. There is an increase in cortisol synthesis capacity and elevated levels of stress modulators. These adaptations enhance the larva's capability to regulate GC levels, preventing excess cortisol while facilitating its production in response to familiar stress.

755 **Figure 1**

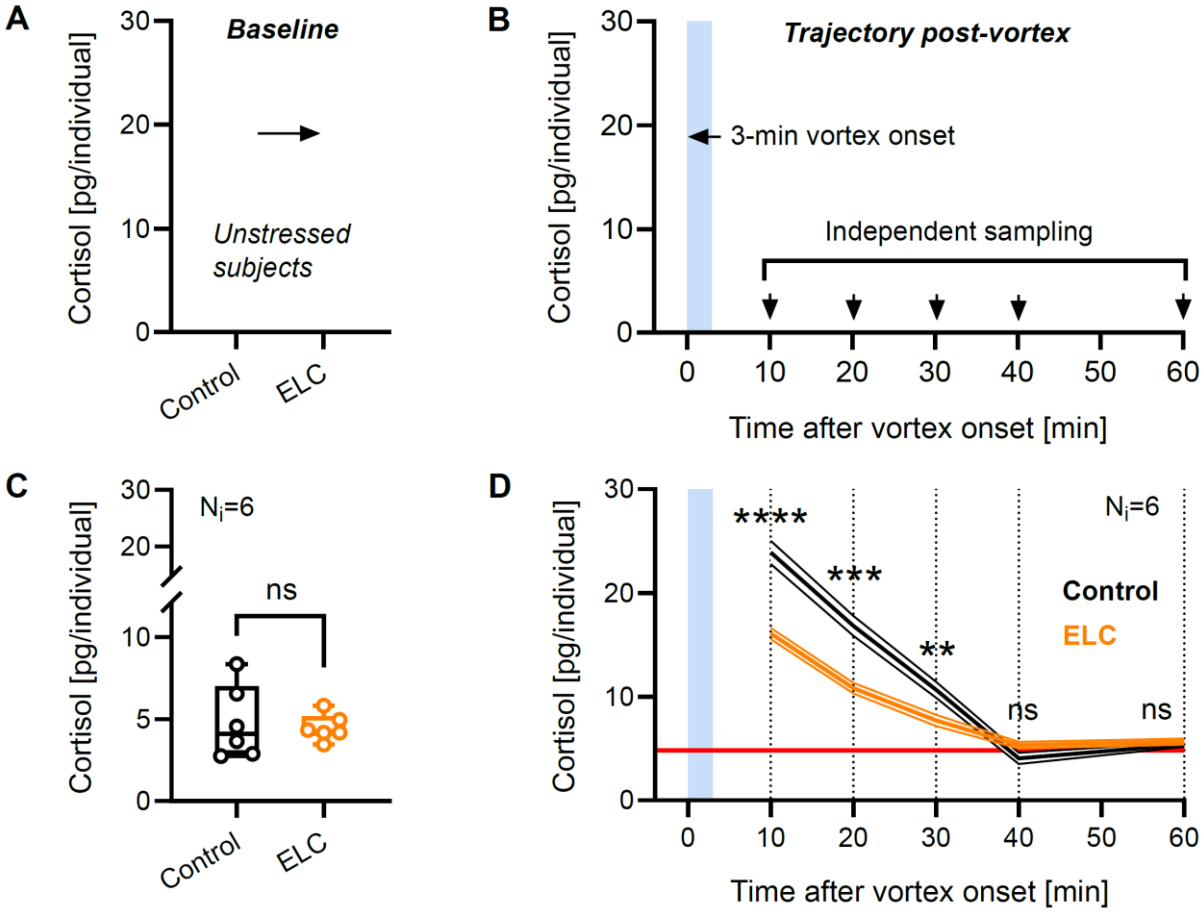
A
Baseline
Unstressed subjects
Cortisol [pg/individual]
30
20
10
0
Control
ELC
B
Trajectory post-vortex
3-min vortex onset
Independent sampling
Cortisol [pg/individual]
0
10
20
30
40
50
60
Time after vortex onset [min]
C
N_i=6
ns
Cortisol [pg/individual]
30
20
10
5
0
Control
ELC
D
N_i=6
****
***
**
ns
ns
Control
ELC
Cortisol [pg/individual]
Time after vortex onset [min]

Figure 2

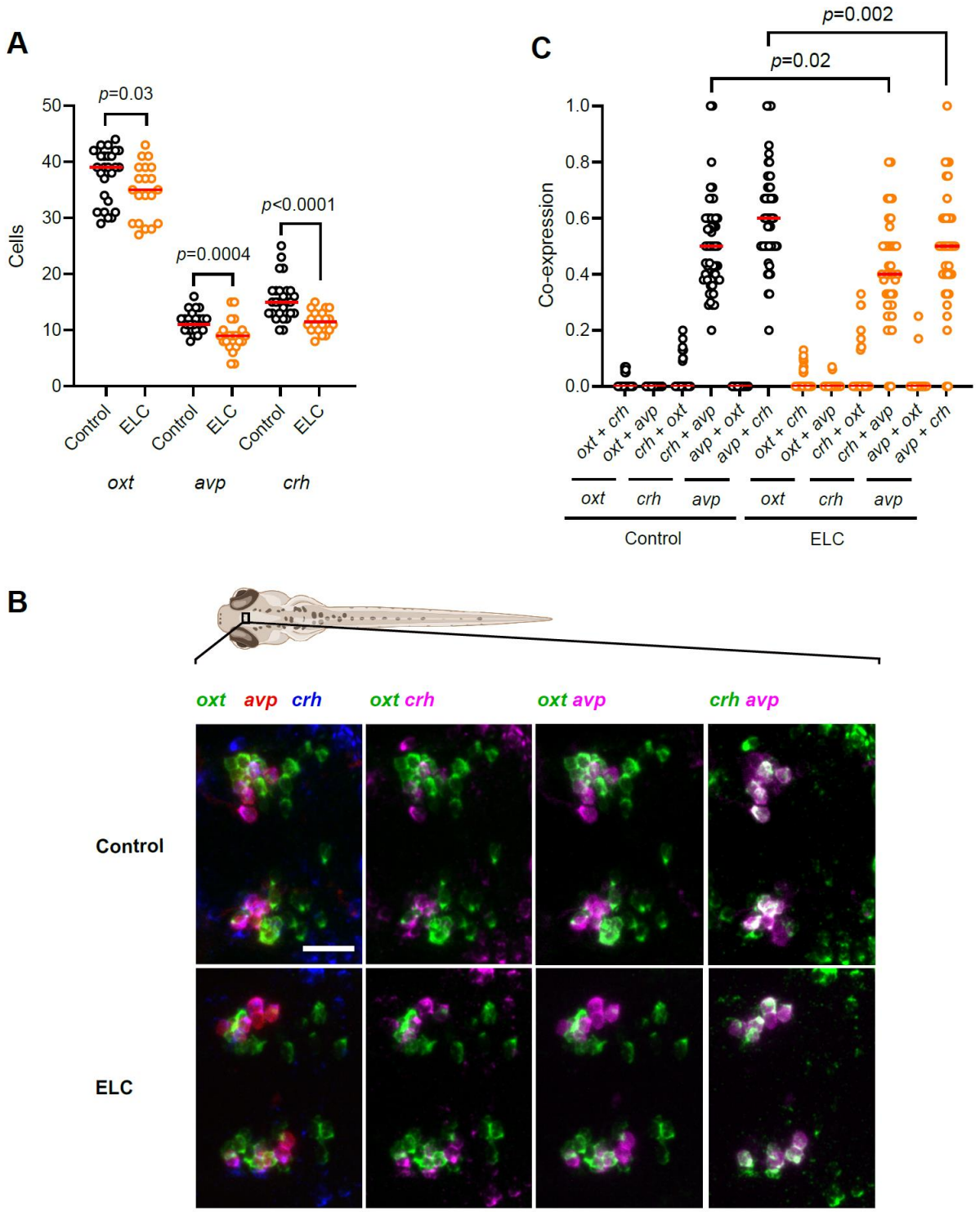
A
p=0.03
p=0.0004
p<0.0001
Cells
50
40
30
20
10
0
Control
ELC
Control
ELC
Control
ELC
oxt
avp
crh
C
p=0.002
p=0.02
Co-expression
1.0
0.8
0.6
0.4
0.2
0.0
oxt + crh
oxt + avp
crh + oxt
crh + avp
avp + oxt
avp + crh
oxt + crh
oxt + avp
crh + oxt
crh + avp
avp + oxt
avp + crh
oxt
crh
avp
oxt
crh
avp
Control
ELC
B
oxt avp crh
oxt crh
oxt avp
crh avp
Control
ELC

757 **Figure 3**

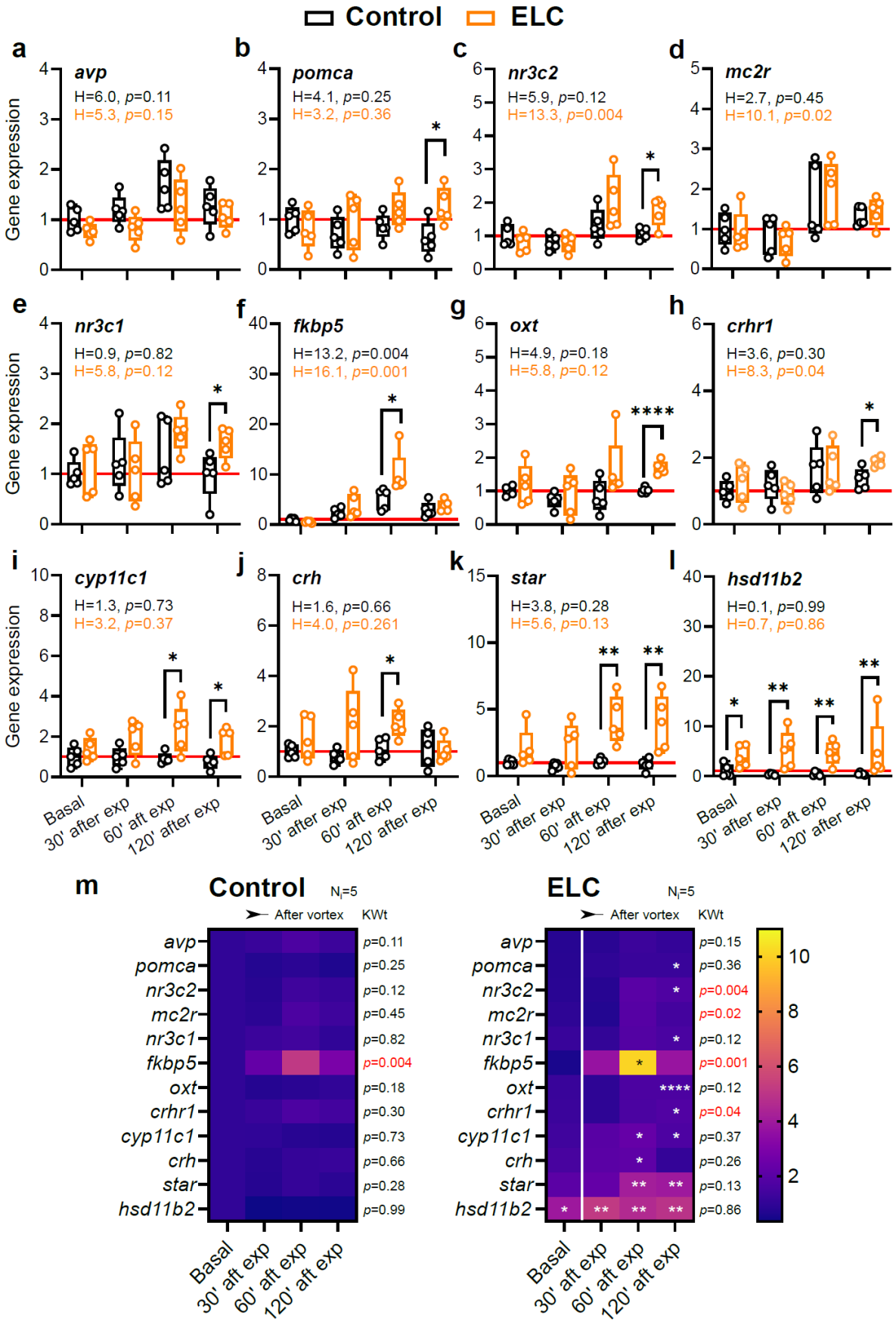
Control
ELC
a
avp
H=6.0, p=0.11
H=5.3, p=0.15
b
pomca
H=4.1, p=0.25
H=3.2, p=0.36
c
nr3c2
H=5.9, p=0.12
H=13.3, p=0.004
d
mc2r
H=2.7, p=0.45
H=10.1, p=0.02
e
nr3c1
H=0.9, p=0.82
H=5.8, p=0.12
f
fkbp5
H=13.2, p=0.004
H=16.1, p=0.001
g
oxt
H=4.9, p=0.18
H=5.8, p=0.12
h
crhr1
H=3.6, p=0.30
H=8.3, p=0.04
i
cyp11c1
H=1.3, p=0.73
H=3.2, p=0.37
j
crh
H=1.6, p=0.66
H=4.0, p=0.261
k
star
H=3.8, p=0.28
H=5.6, p=0.13
l
hsd11b2
H=0.1, p=0.99
H=0.7, p=0.86
Gene expression
Basal
30' after exp
60' aft exp
120' after exp
m
Control
ELC
N=5
After vortex
KWt
avp
pomca
nr3c2
mc2r
nr3c1
fkbp5
oxt
crhr1
cyp11c1
crh
star
hsd11b2
p=0.11
p=0.25
p=0.12
p=0.45
p=0.82
p=0.004
p=0.18
p=0.30
p=0.73
p=0.66
p=0.28
p=0.99
p=0.15
p=0.36
p=0.004
p=0.02
p=0.12
p=0.001
p=0.12
p=0.04
p=0.37
p=0.26
p=0.13
p=0.86

Figure 4

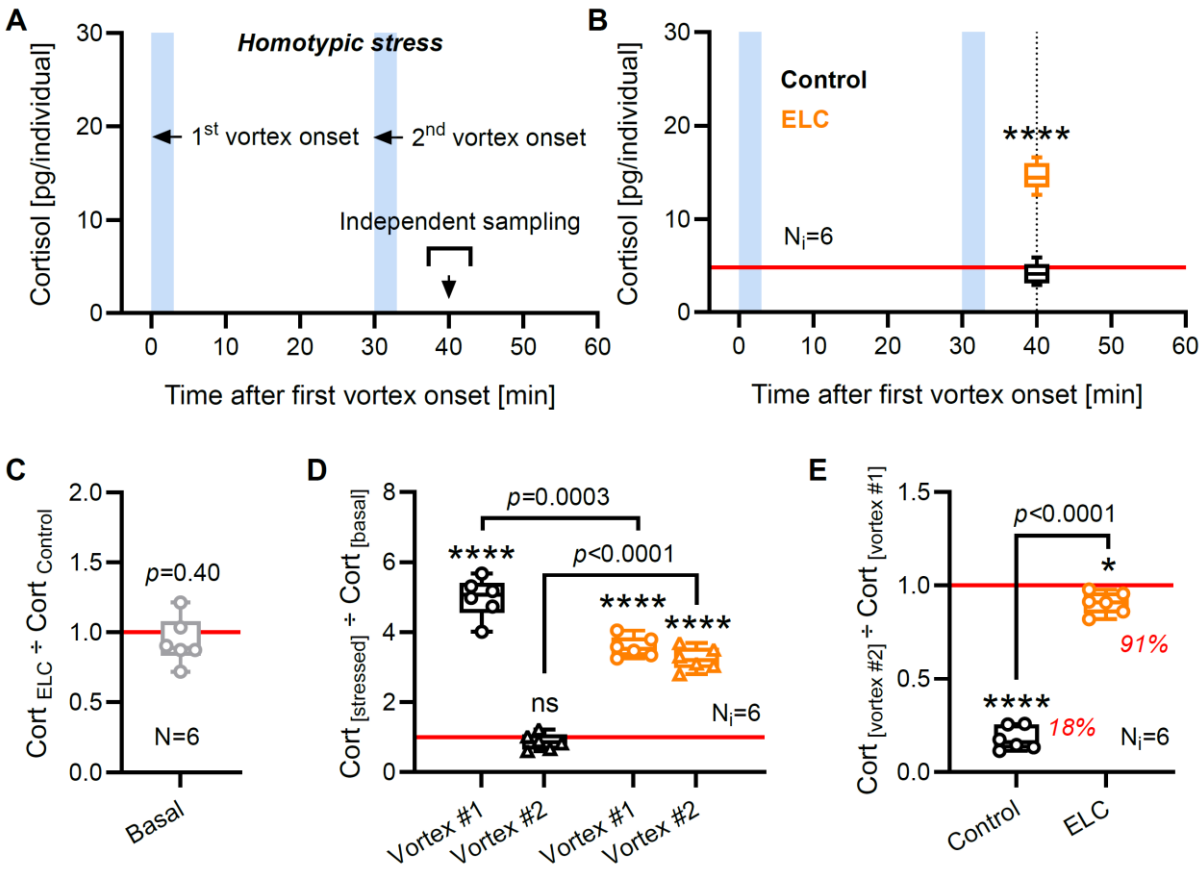
A
Homotypic stress
1st vortex onset
2nd vortex onset
Independent sampling
Cortisol [pg/individual]
Time after first vortex onset [min]
B
Control
ELC
****
Ni=6
Cortisol [pg/individual]
Time after first vortex onset [min]
C
p=0.40
N=6
Cort ELC ÷ Cort Control
Basal
D
p=0.0003
p<0.0001
****
****
****
ns
Ni=6
Cort [stressed] ÷ Cort [basal]
Vortex #1
Vortex #2
Vortex #1
Vortex #2
E
p<0.0001
*
91%
****
18%
Ni=6
Cort [vortex #2] ÷ Cort [vortex #1]
Control
ELC

759 **Figure 5**

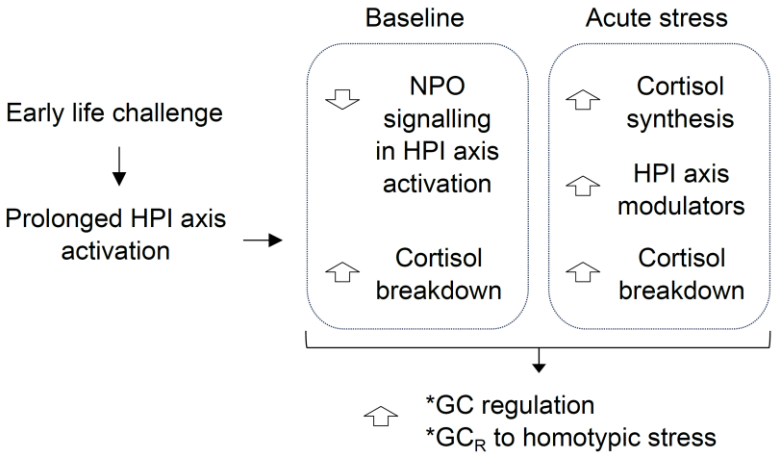
Baseline
Acute stress
Early life challenge
Prolonged HPI axis activation
NPO signalling in HPI axis activation
Cortisol breakdown
Cortisol synthesis
HPI axis modulators
Cortisol breakdown
*GC regulation
*GC$_R$ to homotypic stress

Table 1 Design primer sequences.

Gene name	Gene id	Primer sequence (5′→ 3′)
avp	ENSDARG00000058567	F: CCCAGCCGGAGCCCATCAGA R: CCATGCAGACCTGCGCCTCC
pomca	ENSDARG00000043135	F: CGCAGACCCATCAAGGTGTA R: CGTTTCGGCGGATTCCT
nr3c2	ENSDARG00000102082	F: CCCATTGAGGACCAAATCAC R: AGTAGAGCATTTGGGCGTTG
mc2r	ENSDARG00000054949	F: CTTGGTGATTGTGGCTGTG R: GATAAAGCAGTACATGGGAGAG
nr3c1	ENSDARG00000025032	F: ACAGCTTCTTCCAGCCTCAG R: CCGGTGTTCTCCTGTTTGAT
fkbp5	ENSDARG00000028396	F: CCGACTGCTGTCTTTACCT R: CATGCTGTTTCACAATCTTGC
oxt	ENSDARG00000042845	F: CGGCCTGCTACATCTCAAAC R: TGCCTTCACCACAGCAGATA
crhr1	ENSDARG00000003989	F: TTTATCCTGCGAAATGCCAC R: GCACCAGATCACATTGCTC
cyp11c1	ENSDARG00000042014	F: TGTGCTGAAGGTGATTCTCG R: GCTCATGCACATTCTGAGGA
crh	ENSDARG00000027657	F: ATAGGTGGTGGGTTGTTCC R: CTACATTCATACGGCGGTG
star	ENSDARG00000006137	F: TCAAATTGTGTGCTGGCATT R: CCAAGTGCTAGCTCCAGGTC
hsd11b2	ENSDARG00000001975	F: TGCTGCTGGCTGTACTTCAC R: TGCATCCAACTTCTTTGCTG